

Available online at www.sciencedirect.com

ScienceDirect

Procedia Computer Science 36 (2014) 464 – 469

Procedia
Computer Science

Complex Adaptive Systems, Publication 4
Cihan H. Dagli, Editor in Chief
Conference Organized by Missouri University of Science and Technology
2014-Philadelphia, PA

Simulating Influence of Channel Kinetics and Temperature on Hodgkin-Huxley Threshold Dynamics

George Georgiev^a, Iren Valova^{b*}, Natacha Gueorguieva^c, David Brady^c

^aUniversity of Wisconsin Oshkosh, 800 Algoma Blvd, Oshkosh, WI 54901,

^bUniversity of Massachusetts Dartmouth, 285 Old Westport Rd, N.Dartmouth, MA 02747, USA

^cCollege of Staten Island, City University of New York, 2800 Victory Blvd, Staten Island, NY 10314, USA

Abstract

Information processing in the brain results from the spread and interaction of electrical and chemical signals among neurons. The Hodgkin-Huxley model, describes the spiking and refractory properties of real neurons and serves as a paradigm based on nonlinear conductance of ion channels. Activation of various ion channels establish the spiking behavior of a neuron which determines the communication and coding in nervous system. Firing rates, timing of spikes, and spiking threshold properties are major firing properties of neuronal spiking activities. The temperature influence on neuron spiking threshold regulates the neuronal activities as electrophysiological experiments on neural spiking actions are rarely conducted outside of room temperature in vitro or body temperature in vivo. Temperature changes affect the spiking dynamics of excitable neurons via maximum ion channel conductances and ion channel gating kinetics. The latter has a major impact on changing the shape and amplitude of action potential as well as the generation and propagation of spikes. The purpose of this research is to study, simulate and analyze how the temperature change influence spiking properties of a neuron, channel kinetics as well as activation and inactivation variables of the potassium and sodium channels which determine the dynamics of Hodgkin-Huxley model.

© 2014 The Authors. Published by Elsevier B.V. This is an open access article under the CC BY-NC-ND license (<http://creativecommons.org/licenses/by-nc-nd/3.0/>).

Peer-review under responsibility of scientific committee of Missouri University of Science and Technology

Keywords: brain information processing; spiking neurons; Hodgkin-Huxley model

* Corresponding author. Tel.: 5089998502; fax: 5089999144.

E-mail address: ivalova@umassd.edu

1. Introduction

Brain computations (detection, processing and transmitting of information) are primarily carried out by spiking neurons. The latter communicate with each other via synaptic connections and respond to synaptic stimuli by firing spikes through their axons and dendrites^{1,2}. The inputs to the neuron determine the time of a neuron firing, although the size and shape of the spike are independent from the neuron inputs. Because spiking neural networks are capable of using time as a resource for coding and computations in a very sophisticated way, they are much better suited for applications where the timing of input signals is of importance³.

The responses of a neuron to a given stimulus mostly depend on the cell's mean depolarization level. A time-dependent stimulus may therefore either 1) elicit no spikes at all, 2) generate occasional spikes triggered by transient stimulus elevations, or 3) generate a continuous stream of spikes⁴. While in the first case, the cell depolarization always remains below threshold, in the second case, the average depolarization is near but still below threshold. The latter explains the possibility for large stimulus fluctuations to bring firing from time to time. In the third case, the average depolarization is sufficiently high to maintain the cell above threshold⁵.

Neurons integrate synaptic inputs which depend on the various (voltage- and time-dependent) conductances in the dendrites and soma. The summated signals of these inputs produce action potentials (APs) that are transmitted to other neurons. Threshold which determines the smallest input signal needed to generate a reliable output is an important parameter of any brain subsystem. The question of how subthreshold and suprathreshold stimuli are quantitatively related to the threshold still require a lot of biological and medical studies as well as mathematical modelling and computer simulations.^{6,7}

Temperature changes regulate neuron activities as they have influence on the spiking dynamics of excitable neurons via maximum ion channel conductances and ion channel gating kinetics. The latter has a major impact on changing the shape and amplitude of action potential as well as on the generation and propagation of spikes⁸.

The purpose of this research is to study, simulate and analyze the relationship between threshold and subthreshold and suprathreshold stimuli; threshold dynamics during the membrane depolarization and hyperpolarisation as well as influence of thermal factors on threshold dynamics.

2. Hodgkin-Huxley model

The Hodgkin and Huxley (HH) model⁹ captures the basic mechanism of generating action potentials in the axon. This mechanism is essentially preserved in higher organisms. HH model is described by the following equation:

$$C \frac{dV_m}{dt} = I_{ion} + I(t) \quad (1)$$

where C is the membrane capacity, I_{ion} is the sum of all participating ionic currents that pass through the cell membrane, and $I(t)$ is the applied current. Therefore

$$I_{ion} = \sum_k I_k(t) = \sum_k g_k (E_k - V_m) \quad (2)$$

where each individual ionic component I_k has an associated conductance value g_k and a reversal (equilibrium potential) E_k . The latter represents the potential for which the net ionic current passing through the membrane is zero.

The HH mathematical model (3) includes the following three types of currents: sodium current I_{Na} , potassium current I_K and leakage current I_l (mainly due to chloride ions), i.e.

$$I_{ion} = I_{Na} + I_K + I_l \quad (3)$$

$$\text{or} \quad I_{ion} = g_l(E_l - V_m) + g_{Na}(E_{Na} - V_m) + g_K(E_K - V_m) \quad (4)$$

where C is the membrane capacitance. Each member $g_i(E_i - V_m)$ describes the ionic current resulting from the potential difference $(E_i - V_m)$. The conductance g_l is constant and g_{Na} and g_K are time and voltage dependent. Generally, when environmental temperature T increases, the ionic conductance increases as well and the channel

gating kinetic speeds up, i.e., the time constant of gating variable decreases with the increased temperature.

Transition between permissible and non-permissible states in the HH model satisfies the first-order kinetics in

$$\frac{dp_i}{dt} = \alpha_i(V_m)(1 - p_i) - \beta_i(V_m) p_i \quad (5)$$

where p_i is the probability of gates (channels) of particular type i to be in permissible state and respectively $(1 - p_i)$ is interpreted as the fraction of gates in non-permissible state; voltage-dependent rate constants α_i and β_i describe the transition rates. The fraction of gates in permissible state can reach a steady-state value ($dp_i/dt = 0$ for $t \rightarrow \infty$) if the membrane voltage V_m clamps at the equilibrium potential E_k . The time for approaching the equilibrium potential is given by

$$\tau_i(E_k, T) = \frac{1}{\alpha_i(E_k) + \beta_i(E_k)} \quad (6)$$

when a particular channel is open.

HH includes the probabilities from Eqs. (5) and (6) in modelling the sodium by using three gates of type q and one gate of type h as well as one gate n for potassium conductance. If we denote by G_k the conductance corresponding to channels of type k , it is proportional to individual gate probabilities p_i :

$$G_k(T) = \bar{g}_k(T) \prod_i p_i \quad (7)$$

where $\bar{g}_k(T)$ is the maximal conductance.

The central concept of HH model introduces three state variables that describe the behavior of g_{Na} and g_K and control the opening and closing of ion channels (m controls Na channel opening, h controls Na channel closing, n controls K channel opening) is represented by

$$\sum_k I_k = g_{Na}(T) m^3 h (E_{Na} - V_{Na}) + g_K(T) n^4 (E_K - V_K) + g_l(T) (E_l - V_l) \quad (8)$$

where $0 \leq m, n, h \leq 1$. The empirical differential equations modelling the behaviour of gates $\bar{g}_{Na}(T)$ and $\bar{g}_K(T)$ are

$$\begin{aligned} \frac{dm}{dt} &= \alpha_m(v)(1 - m) - \beta_m(v)m; & \alpha_m(v) &= \frac{0.1(v + 25)}{e^{(v+25)/10} - 1}; & \beta_m(v) &= 4e^{v/18}; \\ \frac{dn}{dt} &= \alpha_n(v)(1 - n) - \beta_n(v)n; & \alpha_n(v) &= \frac{0.01(v + 10)}{e^{(v+10)/10} - 1}; & \beta_n(v) &= 0.125e^{v/80}; \\ \frac{dh}{dt} &= \alpha_h(v)(1 - h) - \beta_h(v)h; & \alpha_h(v) &= 0.07e^{v/20}; & \beta_h(v) &= \frac{1}{e^{(v+30)/10} + 1}; \end{aligned} \quad (9)$$

where v is the voltage across the membrane at a given time.

3. Experiments and results

Since NEURON is designed specifically to simulate the nerve cells, its main advantage is that the user deals directly with concepts that are familiar at the neuroscience level¹⁰. The goal of our experiments is to study the dependence of neuronal spiking activities on spiking threshold properties and the influence of temperature on the dynamics of action potential by observing the rate of depolarization (dV/dt) of the membrane as well as on the threshold rate.

We study: **1.** The effect of different stimuli intensities on voltage change dV/dt versus V_m (the change of voltage just below and after the threshold; **2.** Threshold dynamics determined by the action potential triggered by **a)** excitatory postsynaptic potentials (EPSP) during the depolarization of the membrane; **b)** Inhibitory postsynaptic potentials (IPSP) during the phase of membrane hyperpolarisation. **3.** Influence of thermal factors on threshold

dynamics.

Experiment 1. Subthreshold potential also called a “local response” depolarizes the cell a little bit but it is below the threshold and therefore it does not initiate an action potential (AP) which is a complete reversal of the polarity of the cell. If the stimulus becomes strong enough to pass the threshold potential, then it generates an action potential. This is called the threshold stimulus, which is the weakest stimulus that could generate an AP in a neuron. The stimulus greater than a threshold one is a suprathreshold stimulus.

The goal of the respective simulations is to examine the subthreshold voltage trace, analyzing the rate of change of voltage (dV/dt) versus the voltage (V_m) during the action potential for a timeframe of 12 ms. Partial settings are shown in Fig.1a. For about 8s, the rate of change of voltage V_m is constant and positive, but the voltage dV/dt , which has slowly risen, returns to rest, causing V_m to become negative (Fig.1b). The voltage change depicts depolarization.

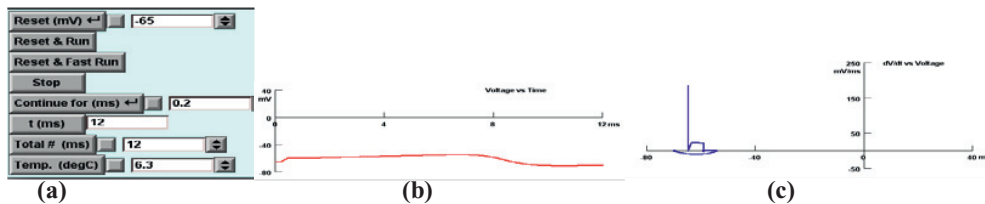


Figure 1. The effect of different stimuli intensities on voltage change

When examining the slope of the subthreshold, a positive stimulus is present (Fig.1c), before flattening from -65 mV to -60 mV. During the pulse, the rate of change declines from 24.3 to 22.2 mV/ms as the voltage rises due to a one-minus-exponential time course to a plateau. There is deviation from a linear voltage rise (Fig.1c). Towards the pulse's end, the rate of change drops to a steady $.95$ mV/ms from the voltage range of -60 mV to -56 mV. The rate of change becomes negative during repolarization before returning positive (around 12 ms). Fig.2a) demonstrates the same simulation under Medium Resolution.

In order to compare the subthreshold to threshold, we increase the amplitude from 39.518 to 39.519 . The subthreshold and suprathreshold have a constant rate of change of about $.95$ mV/ms, but diverge from each other (and the threshold) when either the Na current overcomes the K current and generates an impulse or when the K current is not overtaken, causing the impulse to fail (Fig.2b, c).

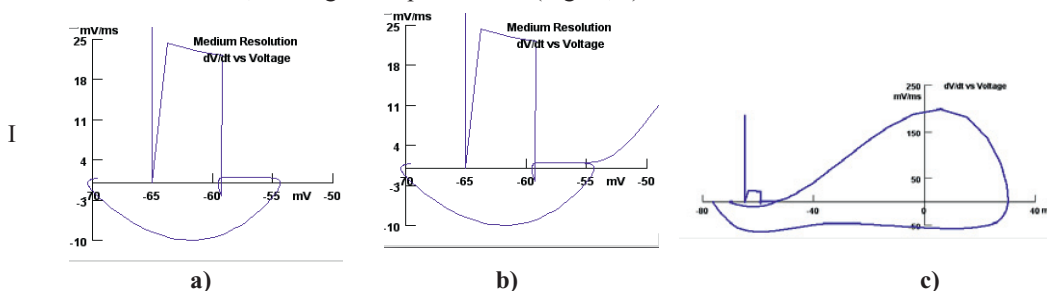


Figure 2. Results of subthreshold and suprathreshold change driven by Na and K currents

Experiment 2a) Simulation of threshold dynamics due to depolarization of the membrane (EPSP). In order to observe the threshold change on action potential triggered by an EPSP, we show one Alpha Synapse panel where the amplitude of conductance set corresponds to a subthreshold 0.59369 ms. The latter was increased to a value of 0.59370 ms (Fig.3a) which is above the threshold. The membrane voltage is driven to the same level by the synaptic current due to increased conductance, along with the square current pulse. Na and K currents compete when approaching threshold due to depolarization, but is after the end of the stimuli (Figs.3b, 4).

Experiment 2b) Simulation of threshold dynamics due to membrane hyperpolarisation (IPSP). Injected currents or inhibitory transmitters can cause impulses at the offset of a hyperpolarization. This “disinhibiting” phenomenon causes an “off-response” and leads to question whether the threshold rate of change of the voltage is the same for both hyperpolarization and depolarization. In order to do this, the amplitude is set to -5.8728 and is then changed to -5.8729 in order to reach the suprathreshold. The pulse duration is set to 5ms with a total number of 25ms. The conductance (g_{max}) is set to zero to prevent the EPSP (Fig.5). The threshold change during membrane hyperpolarization (IPSP).

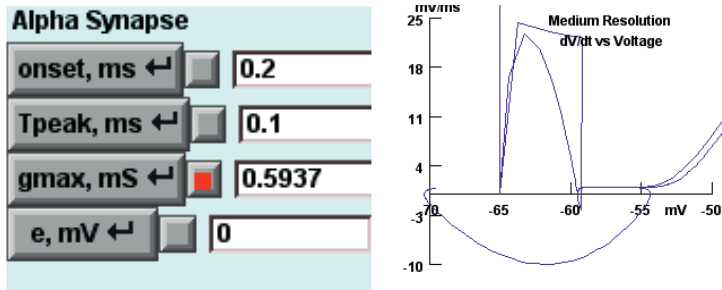


Figure 3. Some Alpha panel setting and plotted median resolution dv/dt vs V_m

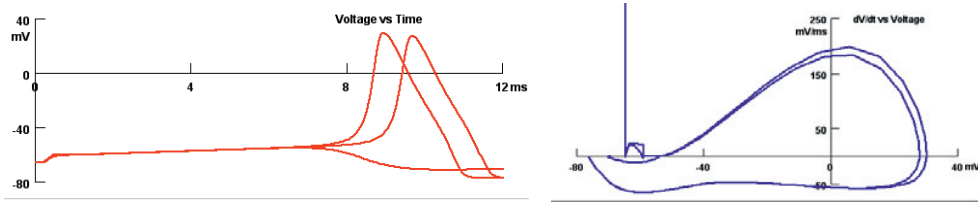


Figure 4. Simulation of threshold dynamics due to membrane depolarization (EPSP)

The longer duration allows the simulation to surpass the threshold unless the conductance is decreased. The conductance was set to 0 when analyzing the IPSP in order to keep the simulation at threshold and prevent any EPSP, making the two comparable (Fig.6).

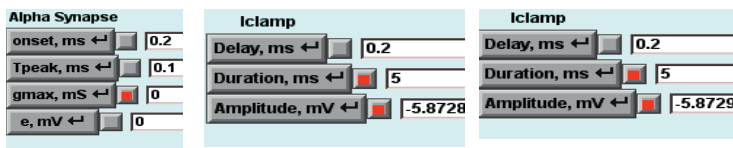


Figure 5. Basic settings for simulating the threshold change during hyperpolarization (IPSP)

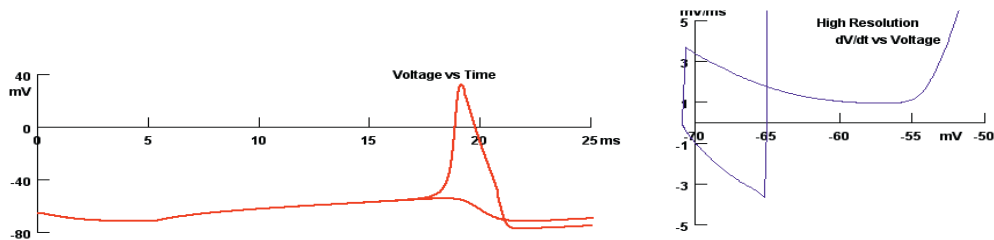


Figure 6. Simulation of threshold dynamics due to hyperpolarization (IPSP)

Experiment 3: Simulating the influence of thermal factors on threshold dynamics. The membrane potential, membrane capacity, environmental temperature, and the activation variable and activation and inactivation variables of the potassium and sodium channels, respectively, form the dynamics of the HH model. With an increase in temperature, there is an increase of ionic conductance and an increase in speed of channel gating kinetics. With the increase of temperature, the kinetics of channel transitions from a closed to open state at a faster speed for depolarization. Inactivation of the Na channels also becomes faster. Raising the temperature leads to faster APs, leaving the question of how much of a faster rate of rise will there be given with the temperature increase. The results for 6.3°C temperature are compared to 26.3°C in order to find the threshold rate of rise (Fig.7). HH⁹ determined that for a 10°C change in temperature the increase in the rate constants for gating the Na and K conductances increase by three times. Temperature was taken at 6.3°C, 10.3°C, 14.3°C, 16.3°C and 26.3°C and the synaptic input changes from a suprathreshold stimulus into a subthreshold stimulus (Fig.7).

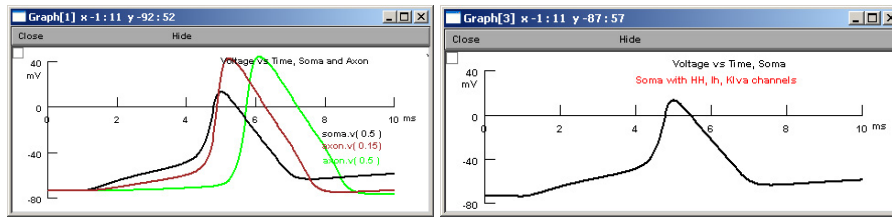


Figure 7. Spiking dynamics of excitable neurons on maximum channel conductances at 6.3°C

Raising the temperature speeds channel kinetics leads to faster action potentials (Fig.8). We observe that a smaller action potential in the soma does not generate a full-blown spike above about 16°C .

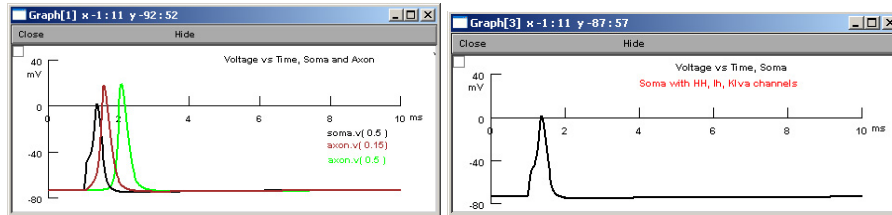


Figure 8. Spiking dynamics of excitable neurons on maximum channel conductances at 26.3°C

4. Conclusions

Our experiments demonstrated that activating the sodium ion channel depolarizes the membrane potential and forms the rise of an action potential whereas the activation of the potassium ion channel along side the inactivation of that of sodium reduces the action potential. This lead to looking at a category where sodium ion channel activation variable m is beneficial for a neuron to spike and a category where a sodium ion channel inactivation variable h and potassium activation variable n terminates action potentials, where comparisons of these categories and environmental temperature dependencies on spiking thresholds can be made. Our simulations confirm the existence of association between thermal factors and channel kinetic behaviors where a specific range of temperatures in the environment could be considered as optima.

References

1. Gerstner W., Coding Properties of Spiking Neurons: Reverse and Cross Correlations. *Neural Networks*, 14:599-610, 2001.
2. Maas W., Networks of spiking neurons: the third generation of neural network models" *Neural Networks*, 10(9):1659-1671, 1998.
3. I. Valova, N. Gueorguieva, F. Troesch, O. Lapteva, *Modeling of Inhibition / Excitation Firing in Olfactory Bulb through Spiking Neurons*. Journal of Neural Computing and Applications, Springer Verlag, Volume 16, Numbers 4-5, May 2007, pp. 355-372(18).
4. I Valova, G. Georgiev, N. Gueorguieva, Conductance Based Neural Simulator: Neural Excitability, Spiking and Bursting. ASME Press Series on Intelligent Engineering Systems Through Artificial Neural Networks (ANNIE 2007), St Louis, MO, pp. 93-99, November 11 – 14, 2007.
5. Schreiber S., Samengo I., Herz A, Two Distinct Mechanisms Shape the Reliability of Neural Responses, *J Neurophysiol* 101: 2239–2251, 2009.
6. Saumil S. Patel, Harold E. Bedell, Dorcas K. Tsang, and Michael T. Ukwade, Relationship between threshold and suprathreshold perception of position and stereoscopic depth, *J Opt Soc Am A Opt Image Sci Vis*. 2009 April; 26(4): 847–861.
7. Nicholas J. Priebe, The relationship between subthreshold and suprathreshold ocular dominance in cat primary visual cortex, *J Neurosci*. 2008 August 20; 28(34): 8553–8559.
8. Shenbing Kuang, Jiafu Wang, Ting Zeng, Aiyin Cao Thermal impact on spiking properties in Hodgkin–Huxley neuron with synaptic stimulus, *Journal of Physics*, Vol. 70, No. 1, 2008, pp. 183-190.
9. Hodgkin, A. and Huxley, A., A quantitative description of membrane current and its application to conduction and excitation in nerve, *J. Physiol. (London)* 117: 500-544, 1952.
10. Hines, ML., Carnevale, N.T., 2000, Expanding NEURON's repertoire of mechanisms with NMODL, *Neural Computation*, 12, pp. 995–1007.